Multivariate Analysis of Multiconductor Transmission Lines for Triple Modal Reservation

Evgeniya Chernikova
Television and Control Department
Tomsk State University of Control Systems and Radioelectronics
Tomsk, Russia

Anton Belousov
Television and Control Department
Tomsk State University of Control Systems and Radioelectronics
Tomsk, Russia

Alexander Zabolotsky
Television and Control Department
Tomsk State University of Control Systems and Radioelectronics
Tomsk, Russia

2021 IEEE 22nd International Conference of Young Professionals in Electron Devices and Materials (EDM) | 978-1-6654-1498-2/21/$31.00 ©2021 IEEE | DOI: 10.1109/EDM52169.2021.9507656

***Abstract*—This article considers two structures of multiconductor transmission lines (MCTL) for triple modal reservation: with a reference conductor in the center and in the form of side polygons. The results of calculating the time and frequency responses of the MCTL in the range of parameters are presented. The calculation of the time response was carried out under various excitations: a trapezoidal pulse signal, electrostatic discharge and a signal from a real ultrashort pulse generator. As a result, deviations for the output waveforms and maximum voltage values were obtained, and a brief analysis of the bandwidth and frequency of the first resonance was performed. By means of parametric optimization of the MCTL by heuristic search, it was possible to reduce the output voltage (from 0.243 V to 0.235 V with an EMF of 1 V) and equalize the time intervals between the decomposition pulses.**

Keywords—electromagnetic compatibility, ultrashort pulse, electrostatic discharge, redundancy, modal reservation, multiconductor transmission lines

I. Introduction

Radioelectronic devices (RED) are an integral part of human life. Since the failure of REDs (especially, the critical ones) can entail various negative consequences, it is important to protect them [1]. An important task in designing REDs is to ensure the electromagnetic compatibility (EMC) [2]. One of the widely used ways to improve the reliability of the critical REDs is cold standby. The principle of its operation is quite simple: if a functioning (reserved) circuit fails, power is supplied to the passive (reserving) circuit [3]. However, reservation approach increases size, weight, power consumption, installation time and cost. Thus, the search for new ways to improve the reliability and ensure EMC of REDs is urgent. Protection against the excitation of powerful ultrashort pulses (USP) is particularly important [4].

In [5], it was first proposed to combine reservation and the effect of modal filtration [6] (decomposition of the exciting USP into a sequence of pulses due to the difference in mode delays) into a single whole, which resulted in modal reservation (MR). Using MR, it is possible to achieve a decrease in the susceptibility of circuits to external conducted emissions and a decrease in the level of conducted emissions from these circuits [7, 8]. One of the characteristics of the MR is the reservation degree, i.e., the ratio of the number of reserving elements to the number of reserved ones [9]. Multiple reservation is used when it is necessary to ensure high reliability rates. For example, with a double MR [10], two additional reserving circuits are used, while three modes come to the output of the multiconductor transmission line (MCTL), and circuits with a triple MR [11] feature three additional reserving circuits and four modes. However, the well-known studies of triple MR are devoted to certain particular aspects, which makes it difficult to objectively compare different MR methods. Meanwhile, it is necessary to assess the possibilities of using MR. The purpose of the present work is to carry out a preliminary comprehensive study of two types of MCTL for a triple MR: with the reference conductor in the center and in the form of side polygons.

The reported study was funded by Russian Science Foundation (project No 20-19-00446) in TUSUR.

II. Simulation Approaches

Simulation and optimization were performed in the TALGAT 2019 software [12]. Initially, cross section geometric models of the MCTLs under study were obtained. Then the matrices of per-unit-length coefficients of electrostatic (**C**) and electromagnetic (**L**) inductions were calculated, as well as per-unit-length resistances (**R**) and conductances (**G**), to take into account losses in conductors [13, 14] and dielectric [15], respectively. Next, equivalent circuits for simulation were compiled, loads (R) and the excitations were set, and the responses to the excitations in the range of parameters were computed.

The cross-sections of the structures under study are shown in Fig. 1, where s is the separation between conductors, w is the width of the conductors, w_1 is the width of the side polygons (in MCTL with the reference conductor in the form of side polygons), t is the thickness of the conductors, h is the thickness of the dielectric, d is the distance from the edge to the conductors (for Fig.1*b* is the distance between the reference and the nearest signal conductor), ε_r is the relative permittivity of the dielectric. The ε_r value is equal to 5 (before optimization) and 4.5 (after optimization) for MCTL on Fig. 1*a* and MCTL on Fig. 1*b*.

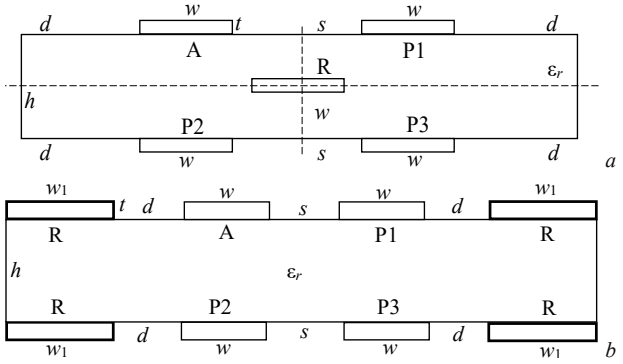

Fig. 1. Cross-section of the MCTL with the reference conductor in the center (*a*) and in the form of side polygons (*b*), where conductors:A is active; P is passive; R is reference

978-1-6654-1498-2/21/$31.00 ©2021 IEEE

Fig. 2*a* shows the equivalent circuit of the MCTLs in general form. The length of the MCTLs (l) is equal to 1 m, and the R values were chosen from the condition of MCTL matching with the path [16]. They are 92 Ω (before optimization) and 50 Ω (after optimization) for the MCTL with the reference conductor in the center and 50 Ω and 105 Ω for MCTL with the reference conductor in the form of side polygons, respectively. To simulate the time response, three sources of excitation were selected: trapezoidal pulse (Fig. 2*b*), electrostatic discharge (ESD) (Fig. 2*c*) and digitized signal of a real USP generator (Fig. 2*d*). When a trapezoidal pulse was applied, an EMF source with an amplitude of 2 V was used with rise, fall, and flat top durations of 50 ps each, so that the total duration was 150 ps. The ESD pulse has a current waveform close to the third severity level with values τ_1=1.56 ns, τ_2=3.87 ns, τ_3=7.77 ns, τ_4=270 ns, I_1=18.56 A, I_2=10.12 A, n=3 according to IEC 61000-4-2. The waveform of the real USP generator is represented by a digitized C9-11 oscilloscope signal with an amplitude of 0.249 V and the rise duration of 312 ps, fall of 259 ps and flat top of 8 ps (by 0.1-0.9 levels) and total pulse duration (by 0.5 level) of 257 ps. Simulation of the frequency response of the MCTL was performed under the harmonic excitation of an EMF source of 2 V in the frequency range from 1 MHz to 3 GHz.

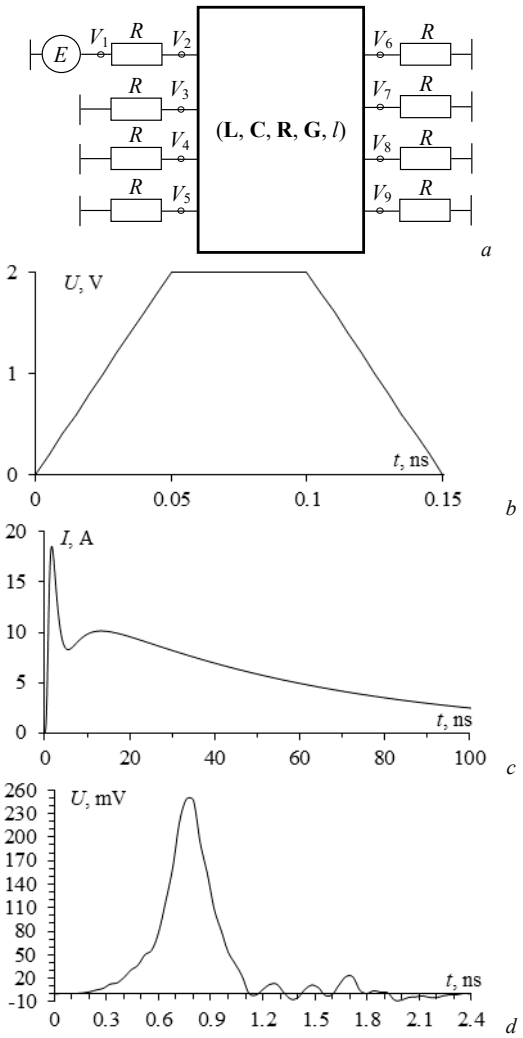

Fig. 2. Equivalent circuit of the considered MCTLs (*a*) and waveforms of the excitating trapezoidal pulse signal (*b*), ESD current (*c*) and digitized real USP signal (*d*)

Because of the symmetry of the MCTLs under consideration, a limitation on the number of optimized parameters is introduced when they are optimized. For example, changing the values of the widths of individual conductors will lead to breaking the MCTL symmetry. Besides, the experience of practical MCTL optimization of [17] allows determining with high accuracy how varying values of optimized parameters influence the output voltage waveform (especially in symmetric structures). Thus, because of a small number of optimized parameters and available experience in practical simulation and optimization, there is no need to turn to time-consuming global optimization methods. Therefore, the parametric optimization of the MCTLs was performed using heuristic search, which showed good results. Section III presents the results of the structures under consideration optimization, which made it possible to improve their characteristics.

III. Simulation Results

A. Time Responses

Simulation of the time responses was performed in the range of the cross-section parameters with some deviation of their values relative to parameter set 1 (Table 1).

The voltage waveforms at the MCTL output with the reference conductor in the center and as side polygons for the first, second, and third parameter sets are shown in Fig. 3*a* and *b*, respectively. The maximum values of the MCTL output voltages (U_{max}) and the mode delays (τ_i) calculated in the parameter range are summarized in Table 2.

From Table 2 and Fig. 3 we can see that, for the MCTL with a reference conductor in the center, the difference of cross-section parameter values (sets 2 and 3) from the medium has an insignificant effect on the τ_4 value, and for the MCTL in the form of side polygons – on the τ_2 value. The maximum difference between neighboring values of τ_i when simulated with different sets of parameters for MCTL with a reference conductor in the center is observed at pulse 2 and equal to 0.15 ns/m, and for MCTL with a reference conductor in the form of side polygons – at pulse 3 and equal to 0.125 ns/m. Thus, the maximum deviations of τ_i values are 0.07 ns/m, 0.15 ns/m, 0.06 ns/m and 0.025 ns/m for the MCTL with a reference conductor in the center and 0.12 ns/m, 0.025 ns/m, 0.125 ns/m and 0.07 ns/m for the MCTL with a reference conductor in the form of side polygons. Nevertheless, when the parameter values deviate from the average, the value of U_{max} practically does not change. U_{max} value is the same for all sets of parameters, and therefore MCTLs with the reference conductor in the center and in the form of side polygons can provide attenuation of 4.04 times and 4.18 times relative to the input voltage, respectively.

Further, we consider the cases when the same MCTLs are excited by an ESD and a digitized real USP signal. When simulating the time response to both excitations, a parameter set 1 is chosen.

In the case of the ESD excitation, only its peak «burst» of about 4 ns undergoes modal decomposition (due to the long ESD duration, it is impossible to observe the whole ESD decomposition in the considered MCTLs). The maximum current amplitudes are equal to 8.86 A and 10.42 A for each MCTL, respectively. Fig. 4 shows the current waveforms at the output of the MCTL. It can be seen that the shape of the current at the output remained practically unchanged.

Nevertheless, the output amplitude values of the considered MCTLs decreased by 1.87 A for MCTLs with the reference conductor in the center and by 3.68 A for MCTLs with the reference conductor in the form of side polygons compared to the input amplitude and were equal to 6.99 A and 6.74 A, respectively. Obviously, since the MCTL does not completely match with the path, there occur multiple reflections distorting the original waveform of the ESD current.

Simulation of the MCTL excited by a digitized signal of the real USP was performed taking into account the losses in the conductors and dielectric (in contrast to simulation when other two excitings are used) with dielectric loss tangent tgδ at a frequency of 1 MHz equal to 0.018 (for ε_r value 4.5) and 0.025 (for ε_r value 5). The voltage waveform at the MCTL output is shown in Fig. 5. Since the total duration of the excitation USP is longer than the maximum value of the difference of the per-unit-length delays ($\Delta\tau$), there is a partial overlapping of decomposition pulses, due to which it is impossible to estimate the τ_i values. Nevertheless, it is possible to estimate the value of U_{max}, which is 0.034 V and 0.043 V for the MCTL with a reference conductor in the center and as side polygons, and the attenuation factor is 7.32 and 5.79 times relative to the input voltage, respectively.

B. Frequency Responses

The frequency responses at the MCTL output with the reference conductor in the center and as side polygons were obtained for 3 sets of parameters and are presented in Fig. 6. The bandwidths at minus 0.707 (Δf) and first resonance frequencies f_1 are summarized in Table 2. The simulation results show that the bandwidth of the MCTL varies insignificantly for all parameter sets (the deviation does not exceed 0.006 GHz and 0.004 GHz for each MCTL). The first resonance frequency at different parameter sets also differs slightly (0.04 GHz and 0.06 GHz for parameter sets 1-3 for each MCTL, respectively).

C. Parametric Optimization

In the optimization, the s and w values varied in the range of 50-2000 μm; t – in the range of 18-175 μm; h – in the range of 200-3000 μm; and d – in the range of 200-2000 μm. As a result of optimization, the parameters for the MCTL with a reference conductor in the center were obtained: s=510 μm; w=1600 μm; t=18 μm; h=500 μm; d=1600 μm. The voltage waveform at the output of the structure is shown in Fig. 7*a*. Optimized parameters for the MCTL with a reference conductor in the form of side polygons are the following: s=220 μm; w=500 μm; w_1=1600 μm (not changed); t=18 μm; h=300 μm; d=800 μm. The voltage waveform at the output of the above structure after optimization is shown in Fig. 7*b*. The value of U_{max} has not undergone changes (before and after optimization it was 0.248 V) because the pairwise equalization of amplitudes of pulses 1, 3 and 2, 4 (caused by symmetry) has been achieved in advance. However, as a result of optimization it was possible to equalize the time intervals between the decomposition pulses so that the values of $\Delta\tau_i$ are 0.49 ns/m, 0.51 ns/m, and 0.49 ns/m. For the MCTL with a reference conductor in the form of side polygons, the value of U_{max} was 0.235 V (before optimization it was 0.243 V). The increased attenuation was achieved by pairwise equalization of 1, 3 and 2, 4 pulses. In addition, it was possible to equalize the time intervals between the decomposition pulses so that the values of $\Delta\tau_i$ are 0.51 ns/m, 0.505 ns/m, and 0.54 ns/m.

IV. Discussion of Results

As a result of the study, it was found that when simulated in the range of specified parameters, the deviations of U_{max} values are insignificant, and the values of Δf and f_1 are very close. Meanwhile, the simulation achieved attenuation (relative to the input voltage) with a reference conductor in the center and as side polygons: trapezoidal pulse by 4.04 and 4.18 times; ESD by 1.32 and 1.37 times, and the pulse of the real USP generator by 7.32 and 5.79 times, respectively. As a result of optimization by heuristic search it was possible to equalize the time intervals between the decomposition pulses for both MCTLs and increase the output voltage attenuation for the MCTL with reference conductor in the form of side polygons (from 0.243 V to 0.235 V). For the MCTL with reference conductor in the center, this value has not changed because pairwise equalization of pulse amplitudes was known to be achieved by the structure symmetry.

TABLE I. Cross-Section Parameter Sets

Structure with a reference conductor	Parameter sets	Parameters			
		s, μm	w, μm	t, μm	h, μm
In the center	1	400	300	105	300
	2	450	350	140	350
	3	350	250	70	250
In the form of side polygons	1	510	1600	35	500
	2	550	1650	70	550
	3	450	1550	18	450

TABLE II. Results of Calculating the Time and Frequency Responses

Structure with a reference conductor	Parameter sets	Parameters						
		U_{max}, V	τ_1, ns/m	τ_2, ns/m	τ_3, ns/m	τ_4, ns/m	Δf, GHz	f_1, GHz
In the center	1	0.2473	5.089	5.471	6.165	7.146	0.148	0.718
	2	0.2473	5.061	5.409	6.142	7.154	0.145	0.701
	3	0.2471	5.128	5.560	6.199	7.135	0.151	0.741
In the form of side polygons	1	0.2437	4.479	4.907	5.873	6.402	0.143	0.331
	2	0.2435	4.538	4.914	5.797	6.367	0.145	0.391
	3	0.2435	4.414	4.890	5.923	6.434	0.141	0.348

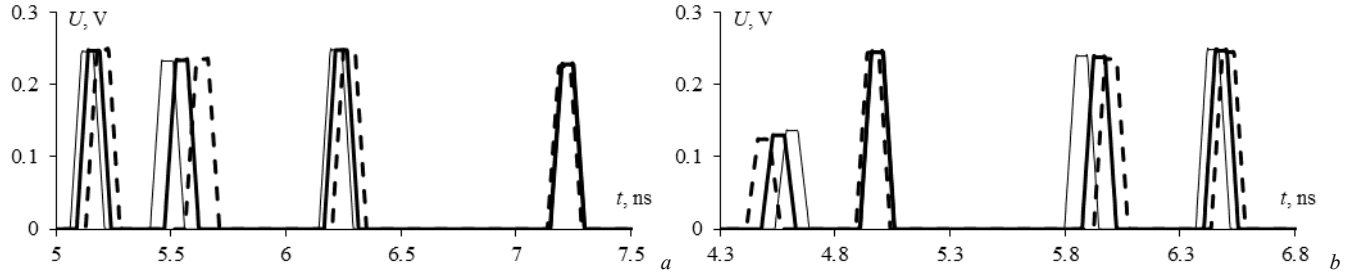

Fig. 3. Voltage waveforms at the MCTL output with the reference conductor in the center (*a*) and in the form of side polygons (*b*) at parameter sets 1 (——), 2 (—) and 3 (– –)

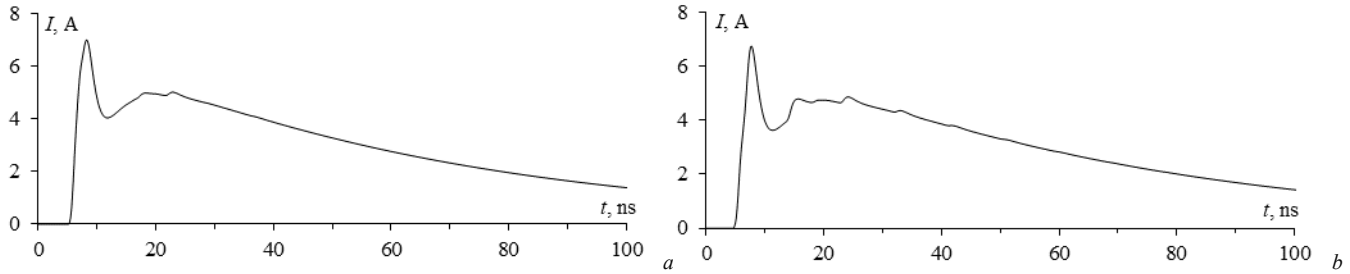

Fig. 4. Current waveforms at the MCTLs output with the reference conductor in the center (a) and as side polygons (b) when excitated by ESD

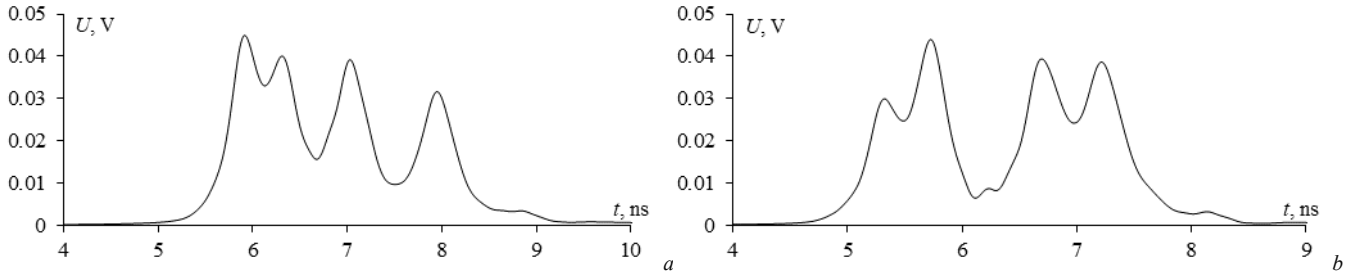

Fig. 5. Voltage waveforms at the MCTL output with the reference conductor in the center (*a*) and in the form of side polygons (*b*) when excitated by a signal from the USP generator

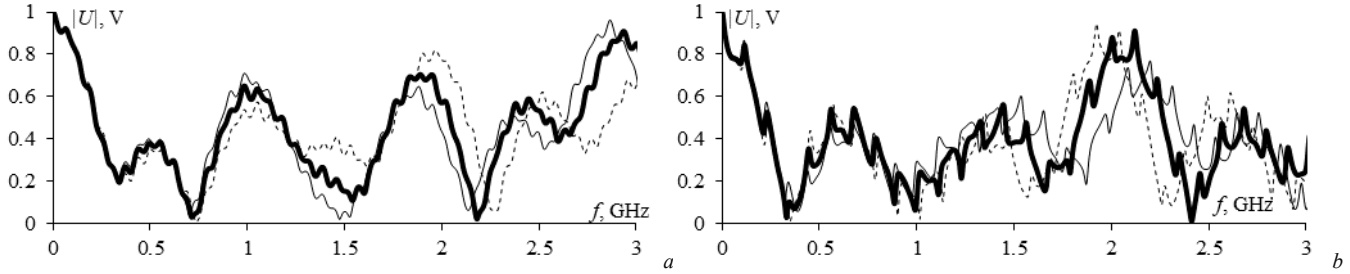

Fig. 6. Frequency responses of the MCTL with the reference conductor in the center (*a*) and in the form of side polygons (*b*) at parameter sets 1 (——), 2 (—) and 3 (– –)

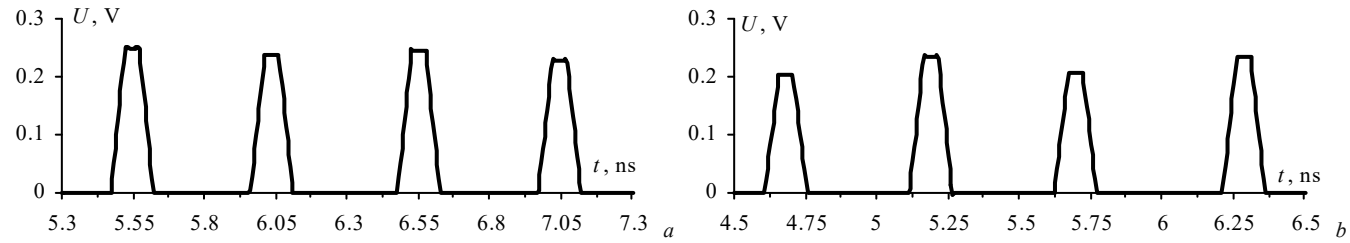

Fig. 7. Voltage waveforms at the MCTL output with the reference conductor in the center (*a*) and in the form of side polygons (*b*) after optimization

V. CONCLUSION

Thus, the MCTLs with the reference conductors in the center and in the form of side polygons for triple MR were studied. A computational experiment and parametric optimization were performed, which showed good results. As a result of simulation and optimization, it was found that both MCTLs can be successfully used to design new devices with triple MR because structurally and technologically their development and manufacture is entirely feasible.

REFERENCES

[1] Z.M. Gizatullin and R.M. Gizatullin, "Investigation of the immunity of computer equipment to the power-line electromagnetic interference," Journal of Communications Technology and Electronics, no. 5, pp. 546–550, 2016.

[2] M. Kučera and M. Šebök "Electromagnetic compatibility analysing of electrical equipment," Diagnostic of electrical machines and insulating systems in electrical engineering (DEMISEE), 2016, pp. 1–6.

[3] T. Van Acker and D. Van Hertem, "Redundancy dependence in the context of competing risks and dynamic degradation," IEEE Transactions on Reliability, pp. 1–9, 2020.

[4] N. Mora, F. Vega, G. Lugrin, F. Rachidi, and M. Rubinstein, "Study and classification of potential IEMI sources," System and assessment notes, note 41, 2014, 92 p.

[5] T.R. Gazizov, P.E. Orlov, A.M. Zabolotskiy, and E.N. Buichkin, "New method of routing of the printed conductors of redundant circuits," Proceedings of TUSUR University, no. 3, pp. 129–131, 2015.

[6] A.T. Gazizov, A.M. Zabolotsky, and T.R. Gazizov, "UWB pulse decomposition in simple printed structures," IEEE Transactions on Electromagnetic Compatibility, vol. 58, no. 4, pp. 1136–1142, 2016.

[7] A.V. Medvedev, V.R. Sharafutdinov, "Using modal reservation for ultrashort pulse attenuation after failure," Proc. of IEEE 2019 International multi-conference on engineering, computer and information sciences (SIBIRCON), 2019, pp 1–4.

[8] A.V. Medvedev, T.R. Gazizov, and Y.S. Zhechev, "Evaluating modal reservation efficiency before and after failure," Journal of Physics: Conference Series, pp. 1–4, 2020.

[9] IEC 60050-192 International electrotechnical vocabulary. Part 192: Dependability, 2015.

[10] A.O. Belousov, E.B. Chernikova, M.A. Samoylichenko, A.V. Medvedev, A.V. Nosov, T.R. Gazizov, and A.M. Zabolotsky, "From symmetry to asymmetry: the use of additional pulses to improve protection against ultrashort pulses based on modal filtration," Symmetry, vol. 11(7), no. 883, pp. 1–38, 2020.

[11] V.R. Sharafutdinov and T.R. Gazizov, "New method for triple reservation of interconnects," Proceedings of TUSUR University, no. 2, pp. 26–30, 2019.

[12] S.P. Kuksenko, "Preliminary results of TUSUR University project for design of spacecraft power distribution network: EMC simulation," IOP Conf. Series: Materials Science and Engineering, vol. 560, no. 012110, pp. 1–7, 2019.

[13] G.L. Matthaei and G.C. Chinn, "Approximate calculation of the high-frequency resistance matrix for multiple coupled lines," Microwave Symposium Digest, 1992, pp. 1353–1354.

[14] R.R Musabaev, "Algorithm for calculating the per-unit-length resistance matrix of a multi-conductor transmission line [Algoritm vychisleniya matricy pogonnyh soprotivlenij mnogoprovodnoj linii peredachi]," Materials of the All-Russian scientific and technical conference with international participation of students, graduate students and young scientists "Scientific session of TUSUR-2017" [Materialy vserossijskoj nauchno-tekhnicheskoj konferencii s mezhdunarodnym uchastiem studentov, aspirantov i molodyh uchenyh "Nauchnaya sessiya TUSUR-2017"], May 2017, pp. 68–71. (*in Russian*).

[15] A.R. Djordjevich, R.M. Biljic, V.D. Likar-Smiljanic, and T.K. Sarkar, "Wideband frequency-domain characterization of FR-4 and time-domain causality," IEEE Trans. on Electromagnetic Compatibility, vol. 43, no. 4, pp. 662–666, 2001.

[16] A.O. Belousov and T.R. Gazizov, "Systematic approach to optimization for protection against intentional ultrashort pulses based on multiconductor modal filters," Complexity, no. 2018, pp. 1–15, 2018.

[17] E.B. Chernikova, A.O. Belousov, T.R. Gazizov, and A.M. Zabolotsky, "Using reflection symmetry to improve the protection of radio-electronic equipment from ultrashort pulses," Symmetry, vol. 11(7), no. 883, pp. 1–25. 2019.